Investigation of the role of GBF1 in the replication of positive-sense single-stranded RNA viruses

Juliette Ferlin, Rayan Farhat, Sandrine Belouzard, Laurence Cocquerel, Antoine Bertin, Didier Hober, Jean Dubuisson, Yves Rouillé

Title: Investigation of the role of GBF1 in the replication of positive-sense single-stranded RNA viruses

Authors: Juliette Ferlin[1], Rayan Farhat[1,*], Sandrine Belouzard[1], Laurence Cocquerel[1], Antoine Bertin[2], Didier Hober[2], Jean Dubuisson[1] and Yves Rouillé[1]

Affiliations: [1]Center for Infection & Immunity of Lille, Inserm U1019, CNRS UMR-8204, Institut Pasteur de Lille, Université de Lille, Lille, France

[2]Université de Lille, Faculté de Médecine, CHU Lille, Laboratoire de Virologie EA3610, Lille, France

Correspondence: Yves Rouillé, yves.rouille@ibl.cnrs.fr

[*]present address: Inserm U1052, Cancer Research Center of Lyon (CRCL), Université de Lyon (UCBL1), CNRS UMR-5286, Centre Léon Bérard, Lyon, France

Keywords: ADP-ribosylation factor, hepatitis C virus, coxsackievirus B4, human coronavirus 229E, Sindbis virus, yellow fever virus

Subject category: Animal viruses – positive-strand RNA

Word counts: abstract: 223; body of text: 5047

Abbreviations: Arf, ADP ribosylation factor; BFA, brefeldin A; BIG, brefeldin A-inhibited guanine nucleotide-exchange protein for ADP ribosylation factor; CRISPR-Cas9, clustered regularly interspaced short palindromic repeats-CRISPR associated protein 9; COP-I, coat protein complex I; CVB4, coxsackievirus B4; DMEM, Dulbecco's modified Eagle's medium; GBF1, golgi brefeldin A resistant guanine nucleotide exchange factor 1; GCA, golgicide A; GEF, guanine nucleotide-exchange factor; HCV, hepatitis C virus; HCoV-229E, human coronavirus 229E ; hpi, hour(s) post infection; KO, knockout; MTS, 3-(4,5-dimethylthiazol-2-yl)-5-(3-carboxymethoxyphenyl)-2-(4-sulfophenyl)-2H-tetrazolium; SINV, Sindbis virus; VLDL, very low density lipoprotein, YFV, yellow fever virus.

ABSTRACT

GBF1 has emerged as a host factor required for the replication of positive-sense single-stranded RNA viruses of different families, but its mechanism of action is still unknown. GBF1 is a guanine-nucleotide exchange factor for Arf family members. Recently, we identified Arf4 and Arf5 (class II Arfs), as host factors required for the replication of hepatitis C virus (HCV), a GBF1-dependent virus. To assess if a GBF1/class II Arfs pathway is conserved among positive-sense single-stranded RNA viruses, we investigated yellow fever virus (YFV), Sindbis virus (SINV), coxsackievirus B4 (CVB4) and human coronavirus 229E (HCoV-229E). We found that GBF1 is involved in the replication of these viruses. However, using siRNA or CRISPR-Cas9 technologies, the depletion of Arf1, Arf3, Arf4 or Arf5 had no impact on viral replication. In contrast, the depletion of Arfs pairs suggested that class II Arfs could be involved in HCoV-229E, YFV and SINV infection, as for HCV, but not in CVB4 infection. In addition, another Arf pair, Arf1 and Arf4, appears essential for YFV and SINV infection, but not for other viruses. Finally, CVB4 infection was not inhibited by any combination of Arf depletion. We conclude that the mechanism of action of GBF1 in viral replication appears not to be conserved, and that a subset of positive-sense single-stranded RNA viruses from different families might require class II Arfs for their replication.

INTRODUCTION

Positive-sense, single-stranded RNA viruses ((+)RNA viruses) replicate their genome in the cytoplasm of their host cell. Their RNA-dependent RNA polymerase and other non-structural proteins implicated in the replication are found in association with cellular membranes. For a number of (+)RNA viruses, intracellular membranes of the host cells are rearranged during replication and viral replication complexes are associated with these membrane rearrangements. The morphology and origin of these membrane rearrangements appear to vary for different viruses. However, it is possible that some conserved cellular pathways are redirected during the replication of different viruses for the formation and functioning of these membranous replication complexes.

GBF1 has recently emerged as a host factor involved in the replication of (+]RNA viruses of the *Picornaviridae* [1-3], *Coronaviridae* [4], *Flaviviridae* [5,6] and *Hepeviridae* [7] families. GBF1 is a brefeldin A (BFA)-sensitive guanine nucleotide exchange factor (GEF) of Arf family members [8]. Through Arf1 activation, it participates to the regulation of COP-I-dependent vesicular transport, phospholipid metabolism, actin cytoskeleton dynamics at the Golgi, and lipid droplet metabolism [9,10]. GBF1 has 6 conserved domains [11]. Its Arf-GEF activity is catalyzed by the Sec7 domain and is selective for class I Arfs (Arf1-3) and class II Arfs (Arf4 and Arf5) [8,12]. The functions of the other conserved domains are less defined [11,13].

Little is known about the mechanism of action of GBF1 in viral infections. Its Arf-GEF activity appears to be of special importance at the onset of the replication of different viruses [4-7]. Accordingly, GBF1 is temporally recruited to replication complexes at early times of poliovirus replication, but not later on [14]. However, its Arf-GEF activity is not required for the formation of replication complexes-associated membrane rearrangements [1,4,5], suggesting that GBF1 is rather involved in a post-formation step of membrane-associated

77 replication complexes. It has been proposed that GBF1 function in viral infections could be
78 related to the regulation of COP-I, a molecular machinery involved in intracellular transport,
79 which has also been reported to be required for the replication of several (+)RNA viruses [15-
80 19]. GBF1 regulates COP-I vesicle formation by stimulating COP-I recruitment to Golgi
81 membranes through Arf1 activation in a BFA-sensitive manner [9,10]. By analogy, the BFA
82 sensitivity of viral replication has been viewed as an argument for Arf1 involvement. In
83 support to this hypothesis, Arf1 [20], or both Arf1 and Arf3 [3] are activated during
84 enterovirus infection, and siRNA-mediated depletion of Arf1 [4,21] or of both Arf1 and Arf3
85 [3] impairs the replication of diverse (+)RNA viruses. However, an experimental
86 demonstration of the existence of a GBF1-Arf1-COP-I pathway involved in viral replication
87 is still lacking. During poliovirus infection, GBF1 is transiently recruited to replication
88 complexes, but this recruitment is not coupled to COP-I recruitment [14]. Moreover, during
89 poliovirus replication, GBF1 function does not depend on its catalytic Sec7 domain and
90 therefore on its Arf-GEF activity [22], indicating a mechanism of action unrelated to Arf1
91 activation.
92 We previously showed that GBF1 is critical to the replication of hepatitis C virus (HCV) [5],
93 and that its Arf-GEF activity is essential for regulating HCV replication [23]. However, GBF1
94 function in HCV replication is not mediated by Arf1, and is distinct from its regulatory
95 functions of the cellular secretory pathway and of the morphology of the Golgi complex, two
96 cellular processes that are mediated by COP-I. We found that different pairs of Arf proteins
97 are involved in these two functions of GBF1. The Arf1/Arf4 pair is involved in the regulation
98 of the secretory pathway and the Arf4/Arf5 pair in the replication of HCV [23]. In this study
99 we compared the requirement of Arfs for the replication of a series of GBF1-dependent
100 (+)RNA viruses from different families.
101

RESULTS

BFA sensitivity of (+)RNA viruses

To probe for GBF1 dependency, we made use of BFA, which inhibits GBF1 and two related Arf-GEFs, named BIG1 and BIG2. In addition to HCV, we selected viruses from different families of (+)RNA viruses, namely yellow fever virus (YFV, *Flaviviridae*), human coronavirus 229E (HCoV-229E, *Coronaviridae*), coxsackievirus B4 (CVB4, *Picornaviridae*), and Sindbis virus (SINV, *Togaviridae*). We also included human adenovirus-5, a DNA virus, as a negative control. Cells were infected in the presence of increasing doses of BFA. To avoid cell toxicity, BFA treatment was restricted to 8 hours of contact, when the infection was scored later than 8 hours post-infection (hpi) (adeno, HCoV-229E, YFV, HCV). As previously shown [5], adenovirus was not inhibited by BFA. In contrast, all RNA viruses tested were sensitive to treatment with 0.1 to 10 μg/ml BFA in a dose-dependent manner (fig. 1a). However, the extent of inhibition was different between viruses. When comparing the inhibition of infection at 1 μg/ml BFA, CVB4 and HCoV-229E appeared the most sensitive viruses (~99% inhibition) and SINV the least one (62% inhibition), HCV and YFV having intermediate sensitivities (~97% and ~88% inhibition, respectively). It is noteworthy that this difference of sensitivity between viruses is only visible in the amplitude of the inhibitory response, but not in the range of inhibitory doses of BFA. For all viruses, the first inhibitory dose was 0.1 μg/ml. No inhibition could be observed with 0.01 μg/ml BFA for any virus. Such a similar range of inhibitory doses observed with all RNA viruses suggests a similar mode of action of BFA against all these viruses.

An MTS assay was performed to quantify the impact of BFA toxicity on Huh-7 cells (fig. 1b). Two protocols were used to assess different protocols of infection. The assay was performed either after 6 hours of contact in the presence of BFA, or after 8 hours of contact followed by

22 hours without BFA. These two protocols correspond to the shortest (CVB4 and SINV) and longest (HCV) infection periods used for quantifying BFA inhibition of viral infections. The only experimental condition showing an inhibition of cell growth or metabolism was with 8 hours incubation with 10 μg/ml BFA, followed by 22 hours without BFA. However, the decrease was not in the same proportion as viral infection inhibitions measured in the same condition. With 1 μg/ml BFA, the inhibition of cell growth was minimal (~20% decrease), whereas the inhibition of viral infections was close to maximal. These results, together with the absence of inhibition of adenovirus infection, indicate that the inhibition of (+)RNA viruses infections could not be explained by BFA toxicity.

GBF1 dependency of (+)RNA viruses

Because GBF1 is not the only target of BFA, we also assessed the impact of BFA on viral infections in R1 cells. R1 cells are Huh-7-derived cells that have a point mutation in one copy of the GBF1 gene [24]. This mutation replaces the methionine residue 832 in the catalytic Sec7 domain by a leucine, a substitution that dramatically decreases BFA binding to GBF1 [25]. Since the two other BFA-sensitive Arf-GEFs, BIG1 and BIG2, are not mutated in R1 cells, any effect of a BFA treatment can be attributed to the inhibition of BIG1 and/or BIG2, but not of GBF1. Inversely, an action of BFA in Huh-7 cells that is not reproduced in R1 cells indicates an involvement of GBF1. We infected R1 cells in the presence of BFA and quantified infections as we did before in Huh-7 cells. A ~100 fold decrease of BFA sensitivity of all viral infections was observed (fig. 2a). The only inhibitory dose was 10 μg/ml, and its impact on infections was similar to that observed with 0.1 μg/ml in Huh-7 cells. This shift in BFA sensitivity between R1 and parental Huh-7 cells indicates an involvement of GBF1 in viral infections.

To further assess the importance of GBF1 in the infection of BFA-sensitive RNA viruses, we used golgicide A (GCA), which is a specific inhibitor of GBF1, with no action on other BFA targets [26]. GCA inhibited all BFA-sensitive viruses (fig. 2b), confirming that the observed inhibition of infection by BFA was only due to its action on GBF1. Again, CVB4 and HCoV-229E were the two most affected viruses. As for BFA treatments, a small decrease in cell growth was also observed with an 8-hour treatment with GCA followed by 22 hours with no inhibitor and, to a lesser extent, with a 6-hour treatment (fig. 2c). These results confirm the implication of GBF1 in the infection of all RNA viruses tested in this study.

We next investigated which step of the viral life cycle is affected by GBF1 inhibition. GBF1 was previously shown to be involved in a post-entry step of the HCV life cycle [5]. CVB4 and HCoV-229E, the two viruses the most affected by BFA, were investigated. To test GBF1 involvement during virus entry, BFA was added to cells during virus contact and removed post-entry. To test GBF1 involvement at a post-entry step, cells were infected in the absence of BFA, and BFA was added during 6 hours after virus removal. For both viruses, the infection was inhibited when BFA was present at the post-entry step, but much less affected when BFA was present at the entry step (fig. 3). These results indicated that GBF1 is likely involved in a post-entry step of the life cycle of these (+)RNA viruses.

Involvement of Arf family members in the infection of (+)RNA viruses

We next assessed if the requirement of GBF1 for (+)RNA virus infection translated into an involvement of Arfs. Arf proteins potentially regulated by GBF1 and sensitive to BFA and GCA, namely Arf1, Arf3, Arf4 and Arf5 (human cells have no Arf2), were depleted with pools of synthetic siRNAs. The extent and the specificity of depletion were evaluated using a set of antibodies specific for each Arf protein (fig. 4a). Each siRNA pool specifically depleted the targeted protein with minimal impact on the expression of other Arfs (fig. 4b), except for

two effects: Arf4 was overexpressed in cells depleted of Arf1, and Arf3 expression was slightly reduced in cells depleted of Arf4 (fig. 4c). Arf4 overexpression in Arf1-depleted cells was previously detected at the mRNA level [23], suggesting that these two Arf proteins are functionally linked. Other variations of expression levels appeared non-significant.

When siRNA-treated cells were infected, an inhibition of infection of approximately 10-30% was measured for all viruses and for all Arf proteins (fig. 4d), except for CVB4, which was not impacted by Arf4 and by Arf5 depletions. The inhibition of HCoV-229E and HCV infection imposed by Arf1, Arf4 and Arf5 siRNAs appeared significant, but most of the other inhibitions were not. Such a moderate and non-specific inhibition of infection in cells depleted of each Arf protein was previously observed with HCV [23]. When Huh-7 cells were depleted of two Arf proteins simultaneously, two pairs of siRNA pools induced an inhibition of infection larger than the ones observed with single depletions (fig. 4e). SINV and YFV infections were inhibited by the depletion of Arf1 and Arf4 (80% and 92% inhibition, respectively). In addition, HCV, SINV and YFV infections were inhibited in cells simultaneously depleted of Arf4 and Arf5 (61%, 70% and 54% inhibition, respectively). HCoV-229E infection also appeared to be reduced in cells depleted of this pair of Arfs, but the inhibition was less dramatic (43% inhibition). In addition, similar inhibitions were also observed with other Arf pairs for this virus. These inhibitions of infection were not correlated to a loss of viability of the cells (fig. 4f). It is noteworthy that CVB4 infection was not strongly affected by any Arf pair depletion. This lack of inhibition was confirmed by immunoblot analysis of VP1 expression (fig. 4g).

To confirm the results obtained using siRNAs, we used CRISPR-Cas9 technology to generate knockout (KO) cells. One Arf4KO, one Arf5KO and three Arf1KO cell lines were generated. To avoid biases resulting from the use of clones, we used the whole population of cells transfected with CRISPR-Cas9 constructs in each case. A small amount of residual expression

of targeted proteins of 0 to 20% was measured for each cell line (fig. 5a). This residual expression likely resulted from the presence of a small amount of cells expressing the targeted protein. No major impact on the expression of other Arfs was observed, except for a slight decrease in Arf5 expression in the Arf1KO cell line 1.3, which was not observed for the two other Arf1KO cell lines (fig. 5b).

ArfKO cell lines were infected with HCoV-229E, HCV, SINV or YFV, the four viruses impacted in siRNA experiments. The infections of these four viruses were marginally affected in the three Arf1KO cell lines. They were inhibited by 20-30% in the Arf5KO cell line 5.1. In the Arf4KO cell line 4.1, HCV infection was inhibited by 20% and the infections by HCoV-229E, SINV and YFV were inhibited by ~50% (fig. 5c). These results confirmed the lack of inhibition of HCV infection by any single Arf depletion, and revealed an importance of Arf4 in HCoV-229E, SINV and YFV infections that was not detected in siRNA experiments.

We next tried to generate double KO cell lines by transfecting Arf4 CRISPR-Cas9 constructs in the Arf5KO cell line or Arf5 CRISPR-Cas9 constructs in the Arf4KO cell line. Unfortunately, most cells died during the selection, and the few surviving cells turned out not to be double KO (data not shown). This indicates that a permanent invalidation of both class II Arf genes is lethal for Huh-7 cells. Therefore, we used siRNAs to transiently deplete Arf proteins in ArfKO cell lines. Again, we observed a strong toxicity of siRNAs to Arf1 or to Arf5 transfected in the Arf4KO cell line. On the other hand, Arf4 depletion by siRNA transfection was also toxic in Arf1KO cells, but not in Arf5KO cells. An MTS assay confirmed the absence of toxicity of Arf4 siRNA transfection in the Arf5KO cell line 5.1 (fig. 6a).

Therefore, we used this experimental setup (siRNA-mediated depletion of Arf4 in Arf5KO cells) to confirm the importance of the pair of class II Arfs in viral infections. As controls, we used a non-targeting siRNA, as for experiments in parental Huh-7 cells, and also the Arf5

siRNA pool, which should have no impact in Arf5KO cells. As a control cell line, we used a cell line selected after transfection of a CRISPR-Cas9 construct expressing no guide RNA. The depletion of Arf4 and Arf5 was confirmed by immunobloting (fig. 6b). Arf5 was undetectable in cells transfected with Arf5 siRNA and in Arf5KO cells, and was not affected by the depletion of Arf4 in control cells. Arf4 expression was reduced to ~30% in both cell lines after transfection of Arf4 siRNA.

siRNA-transfected control and Arf5KO cells were infected with HCoV-229E, HCV, SINV and YFV. As expected from results of previous double depletions by siRNA, HCoV-229E, HCV and SINV infections were strongly inhibited (85%, 89% and 83% inhibition, respectively) (fig. 6c). In contrast, YFV infection was less impacted (53% inhibition). In all other conditions, viral infections were inhibited by less than 40%, except in Arf5KO cells transfected with Arf5 siRNAs, which surprisingly displayed an inhibition of almost 50% of HCV and SINV infections, likely resulting from off-target effects. All together, these results confirmed the importance of class II Arfs for infection by HCV [23] and by HCoV-229E, SINV and YFV, as previously observed with double siRNAs transfection-based experiments.

DISCUSSION

In this study, we investigated whether the function of class II Arfs is conserved in infections of GBF1-dependent (+)RNA viruses. GBF1 has been reported to be required for the replication of different viruses, but its function is still not understood. Recently, we found that the function of GBF1 in HCV replication differs from its function in the early secretory pathway [24]. Whereas the effect of GBF1 inhibition or depletion on the secretion of albumin and VLDL and on the Golgi morphology is phenocopied by simultaneously depleting both Arf1 and Arf4, the depletion of this pair of Arfs has no impact on HCV infection [23]. In contrast, the impact of GBF1 inhibition or depletion on HCV replication is phenocopied by

the depletion of another pair of Arfs. HCV replication is specifically inhibited by simultaneously depleting Arf4 and Arf5. Interestingly, the depletion of this pair of Arfs has no impact on the secretion of albumin or VLDL. Cells depleted of Arf4 and Arf5 accumulate enlarged lipid droplets, suggesting a function related to the regulation of lipid metabolism or, at least, to the morphology of these organelles, which are known to depend on GBF1 for their metabolism [9,10]. Therefore, different GBF1 functions appear to be mediated by different pairs of Arfs. This is in line with a previous report that the depletion of different Arf pairs results in different specific phenotypes on secretory and endosomal compartments [27], which are collectively observed upon BFA treatment of the cells. All these observations suggest that different pairs of Arfs could mediate the different cellular functions that are regulated by GBF1, BIG1 and BIG2, the three BFA-sensitive Arf-GEFs.

The function of the class II Arf pair in virus infection appears to be partly conserved among viruses from different families. Their simultaneous depletion inhibited infection by HCV, HCoV-229E, SINV and YFV, but not by CVB4. Interestingly, all these viruses also depend on GBF1 for their replication, suggesting the existence of a GBF1-Arf4/5 pathway requirement for some but not all (+)RNA viruses. These inhibitions were also observed to some extent with the Arf4KO but not the Arf5KO cell line, suggesting a major importance of Arf4, which had not been observed with siRNA-mediated depletions of individual Arf proteins.

We also tried to confirm the contribution of class II Arfs with double KO cells. Unfortunately, the double KO was not viable, when each single KO was, suggesting that class II Arfs collectively fulfil a vital function in Huh-7 cells. We also observed a great reduction of viability in Arf4KO cells transfected with Arf5 siRNA. Nevertheless, the siRNA-mediated depletion of Arf4 in Arf5KO cells turned out to be not toxic. This difference probably resulted from a less pronounced down-regulation imposed by Arf4 siRNA, than by Arf5

siRNA. Therefore, the transfection of Arf4 siRNA in Arf5KO cells probably resulted in residual Arf4 expression levels compatible with cell survival. This allowed us to confirm the inhibition of HCV, HCoV-229E, SINV and YFV infections in cells depleted of both class II Arfs. Class II Arfs were previously reported to be implicated in the dengue virus life cycle, and more precisely in the assembly/secretion step, but the replication step was not investigated [28]. It would have been interesting to confirm that the depletion of class II Arfs actually affects the replication step of the life cycle of HCoV-229E, SINV and YFV, as it does for HCV [23]. Unfortunately, we do not have the tools to address this question. Nevertheless, we have shown that GBF1 is implicated in HCV replication [5] and in a post-entry step of the life cycle of HCoV-229E and CVB4 (this study).

In addition to the Arf4/Arf5 pair, YFV and SINV were also sensitive to the simultaneous depletion of Arf1 and Arf4. As this Arf pair is involved in the regulation of the secretory pathway [23,27], this suggests an involvement of this pathway in the life cycle of these viruses. Currently, we do not know which step of their life cycle is actually impacted by the depletion of this Arf pair. An entry inhibition can be hypothesized, resulting from a default of expression of specific receptors at the cell surface. Alternatively, we cannot rule out the possibility of an inhibition of the replication step. The Arf1/Arf4 pair has been previously reported to be involved in the localization of the capsid protein to lipid droplets in dengue virus-infected cells [29].

In contrast, CVB4 infection was not inhibited in cells depleted of both Arf4 and Arf5, nor of any other Arf pair, although it was inhibited by BFA in a GBF1-dependent manner. This suggests that the function of GBF1 in CVB4 infection could be unrelated to its Arf-GEF activity. Previously, a study by Lanke et al. demonstrated the implication of GBF1, but could not find any implication of Arfs, in the replication of CVB3 [2]. A sec7-independent GBF1 function has also been reported for poliovirus infection [22]. In contrast, the replication of

enterovirus 71 has been reported to depend on the pair of class I Arfs, Arf1 and Arf3 [3]. Further studies will be necessary to assess if CVB4, and more generally which other enteroviruses use a Sec7-independent function of GBF1 and what is the mechanism of action.

In conclusion, this study confirms and extends the implication of class II Arfs in the infection of different (+)RNA viruses. Cellular pathways specifically controlled by class II Arfs are currently unknown. Arf4 has been proposed to be part of a Golgi stress-response pathway [30]. This function of Arf4 requires GBF1, but is not linked to Arf5. Collectively, class II Arfs are not involved in the regulation of the secretory pathway [23,27]. They fulfil a vital function in Huh-7 cells, and they also appear to be involved in regulating the morphology of lipid droplets. However, we still do not know whether these two functions are related to each other. Future work is required to decipher pathways specifically regulated by class II Arfs and to identify effectors implicated in these pathways, which could be interesting new targets for developing antiviral therapies.

METHODS

Reagents. Dulbecco's modified Eagle's medium (DMEM), phosphate-buffered saline (PBS) and 4',6-diamidino-2-phenylindole (DAPI) were purchased from Life Technologies. Goat and fetal calf sera (FCS) were from Eurobio. Golgicide A and Mowiol 4-88 were from Calbiochem. Protease inhibitors cocktail (Complete) was from Roche. Other chemicals were from Sigma.

Antibodies. Mouse anti-HCV E1 mAb A4 [31] and mouse anti-YFV E mAb 2D12 (anti-E, ATCC CRL-1689) were produced in vitro by using a MiniPerm apparatus (Heraeus). Mouse anti-enterovirus VP1 mAb (clone 5-D8/1) was from DAKO. Mouse anti-Arf1 mAb 1A9/5 was from Santa Cruz Biotechnology. Mouse anti-Arf3 mAb was from BD Biosciences.

Rabbit anti-human Arf4 mAb EPR12133B was from Abcam. Mouse anti-Arf5 mAb 1B4 was from Abnova. Mouse anti-β-tubulin mAb TUB 2.1 was from Sigma. Mouse anti-GFP mAb was from Roche. Peroxidase-conjugated secondary antibodies and cyanine 3-conjugated goat anti-mouse IgG were from Jackson Immunoresearch.

Cell culture. Huh-7 [32] and R1 [24] cells were grown at 37°C in Dulbecco's modified Eagle's medium (DMEM), high glucose modification, supplemented with glutamax-I and 10% FCS.

HCV. The virus JFH1-CSN6A4 used in this study was produced as previously described [5]. For infection assays, cells were infected for 2 hours at 37°C, and fixed with cold methanol at 30 hpi.

Adenovirus. A recombinant defective adenovirus expressing a green fluorescent protein (GFP) was as previously described [24]. Cells were infected for 1 hour at 37°C, and fixed for 20 minutes with PFA 3% at 16 hpi.

SINV. A recombinant Sindbis virus expressing HCV E1 glycoprotein was as previously described [33]. Cells were infected for 1 hour at 37°C, and fixed with cold methanol at 6 hpi.

YFV. Yellow fever virus strain 17D was obtained from Dr Philippe Desprès (Institut Pasteur de Paris). Cells were infected for 1 hour at 37°C, and fixed with PFA 3% at 24 hpi.

HCoV-229E. A recombinant human coronavirus 229E expressing GFP [34] was provided by Dr Volker Thiel (University of Bern, Swiss). Cells were infected for 1 hour at 37°C, and fixed with PFA 3% at 12 hpi.

CVB4. Coxsackievirus B4 strain E2 (CVB4) was previously provided by Dr Ji-Won Yoon (Julia McFarlane Diabetes Research Center, Calgary, Alberta, Canada). CVB4 suspensions were prepared and titred as described [35]. Cells were infected for 1 hour at 37°C, and fixed with cold methanol at 6 hpi.

350 ***Infection assays.*** Huh-7 cells grown on glass coverslips or in 96-well plates were incubated
351 at 37°C for 1 or 2 hours (depending on the virus) in the presence of the virus. For each virus,
352 the viral stocks were diluted so as to obtain 20 to 40% of infected cells in control conditions.
353 Cells were fixed at a time that allows for a clear detection of infected cells vs. non-infected
354 cells, and avoids the detection of reinfection events, thus limiting the analysis to a single
355 round of infection. Cells were fixed for 20 min with 3% PFA or for 1 min with cold methanol
356 at -20°C. Cells were then rinsed with PBS and processed for immunofluorescence as
357 previously described [36] using specific primary mouse antibodies to HCV E1 (for both HCV
358 and SINV), YFV E, GFP (for HCoV-229E) or VP1 (for CVB4) followed by a cyanine-3-
359 conjugated goat anti-mouse IgG secondary antibody for the detection of infected cells. Nuclei
360 were stained with DAPI. Immunostained cells were observed with a Zeiss Axiophot
361 microscope equipped with a 10×-magnification objective. Fluorescent signals were collected
362 with a Coolsnap ES camera (Photometrix). For each well or coverslip, a series of images of
363 randomly picked areas were automatically recorded using the Metamorph software. Cells
364 labeled with anti-virus mAbs were counted as infected cells. The total number of cells was
365 obtained from DAPI-labeled nuclei. Infected cells and nuclei were automatically counted
366 using a macro written in the ImageJ software. Infections were scored as the ratio of infected
367 over total cells. Data are presented as the percentage of infection relative to the control
368 condition.
369 ***Drug treatments.*** BFA and GCA were dissolved in DMSO, aliquoted and kept at -20°C. For
370 infection assays with SINV and CVB4, cells were incubated with BFA or GCA at the
371 indicated concentrations during virus inoculation and up to 6 hpi. For infection assays with
372 HCV, YFV, adenovirus and HCoV-229E, cells were incubated with BFA or GCA at the
373 indicated concentrations during virus inoculation and up to 8 hpi. The medium was then

removed; the cells were rinsed twice with PBS and returned to a drug-free medium until the end of the assay. For each experiment, a control condition with DMSO was included.

RNA interference. RNA interference experiments were performed as previously described [23]. siRNAs were obtained from Dharmacon. For Arf3, Arf4 and Arf5, pools of 4 siRNA were used. For Arf1, a mix of 2 individual siRNAs (J-011580-05-0005 & J-011580-08-0005) was used to avoid off-target effects resulting from the use of the pool of 4 siRNAs [23]. The control siRNA was the non-targeting siRNA #1 (D-001810-01-20). Briefly, cells were transfected with siRNAs at 20 nM using lipofectamine RNAi MAX (Life Technologies). The cells were passed the day after and infected at 3 days post-transfection.

Generation of knock out cells. Arf genes were invalidated in Huh-7 cells using the CRISPR-Cas9 technology. Guide RNA sequences were selected with the help of the CRISPR design tool at http://crispr.mit.edu/ and inserted into pX330-U6-Chimeric_BB-CBh-hSpCas9, a gift from Feng Zhang (Addgene plasmid # 42230). Selected target sequences for sgRNA design were CTTAAGCTTGTAGAGGATCG for Arf1.1, GATCCTCTACAAGCTTAAGC for Arf1.2, ATCCTCTACAAGCTTAAGCT for Arf1.3, GGAGATAGTGAGGCCCATGG for Arf4.1 and GAAGATCCGCGAAAAGAGCG for Arf5.1 KO cell lines. Constructs were generated as described [37]. Sub-confluent Huh-7 cells grown in 6-well plates were transfected with 1 μg of CRISPR-Cas9 construct and 50 ng of pPuro using the TransIT-LT1 transfection reagent (Mirus). Two days later, transfected cells were selected with puromycin at 5 μg/ml during 4 days. The puromycin-containing medium was renewed every day. After 4 days of selection, almost all the cells from control transfections with no pPuro plasmid were dead. Selected cells were then expanded in puromycin-free medium. The residual expression of targeted protein was measured using immunoblotting.

Immunoblotting. Cells were rinsed 3 times with cold PBS, and lysed at 4°C for 20 min in a buffer containing 50 mM TrisCl, pH 7.5, 100 mM NaCl, 2 mM EDTA, 1% Triton- X, 0.1%

SDS, 1 mM PMSF, and a mix of protease inhibitors. Insoluble material was removed by centrifugation at 4°C. The protein content was determined using a bicinchoninic acid assay (Sigma). The proteins were then resolved by SDS-PAGE and transferred onto nitrocellulose membranes (Hybond-ECL; Amersham) using a Trans-Blot apparatus (Bio-Rad). Proteins of interest were revealed with specific primary antibodies, followed by species-specific secondary antibodies conjugated to peroxidase. Proteins were visualized using enhanced chemiluminescence (SuperSignal West Pico Chemiluminescent Substrate from Thermofischer Scientific). The signals were recorded using a LAS 3000 apparatus (Fujifilm). Quantification of unsaturated signals was carried out using the gel quantification function of ImageJ.

Viability assay. An MTS [3-(4,5-dimethylthiazol-2-yl)-5-(3-carboxymethoxyphenyl)-2-(4-sulfophenyl)-2H-tetrazolium]-based viability assay (CellTiter 96 aqueous nonradioactive cell proliferation assay from Promega) was conducted as recommended by the manufacturer using sub-confluent cell cultures grown in 96-well plates.

Statistical analysis. Statistical analysis was performed using the software Prism. The significance between groups was determined by one-way ANOVA and a Dunnett post-hoc test. Only significant p-values are indicated by the asterisks above the graphs.

AUTHOR STATEMENTS

Funding information: This work was supported in part by the French 'Agence Nationale de Recherche sur le Sida et les hépatites virales' (ANRS). JF was supported by a pre-doctoral fellowship from ANRS.

Acknowledgements: The authors thank Dr Philippe Desprès, Dr Volker Thiel and Dr Feng Zhang for providing us with viruses and plasmid. Some data were generated with the help of the imaging core facility of the Institut Pasteur de Lille (BICeL).

Conflicts of interest: The authors declare that no conflict of interest exists

REFERENCES

1. **Belov GA, Feng Q, Nikovics K, Jackson CL, Ehrenfeld E.** A critical role of a cellular membrane traffic protein in poliovirus RNA replication. *PLoS Pathog*. 2008 Nov 1;4:e1000216.

2. **Lanke KHW, van der Schaar HM, Belov GA, Feng Q, Duijsings D, *et al*.** GBF1, a guanine nucleotide exchange factor for Arf, is crucial for coxsackievirus B3 RNA replication. *J Virol*. 2009;83:11940–11949.

3. **Wang J, Du J, Jin Q.** Class I ADP-Ribosylation Factors Are Involved in Enterovirus 71 Replication. Zheng Z-M, editor. *PLoS ONE*. 2014;9(6):e99768.

4. **Verheije MH, Raaben M, Mari M, Lintelo te EG, Reggiori F, *et al*.** Mouse hepatitis coronavirus RNA replication depends on GBF1-mediated ARF1 activation. *PLoS Pathog*. 2008;4:e1000088.

5. **Goueslain L, Alsaleh K, Horellou P, Roingeard P, Descamps V, *et al*.** Identification of GBF1 as a cellular factor required for hepatitis C virus RNA replication. *J Virol*. 2010;84:773–787.

6. **Carpp LN, Rogers RS, Moritz RL, Aitchison JD.** Quantitative proteomic analysis of host-virus interactions reveals a role for Golgi brefeldin A resistance factor 1 (GBF1) in dengue infection. *Mol Cell Proteomics*. 2014;13:2836–2854.

7. **Farhat R, Ankavay M, Lebsir N, Gouttenoire J, Jackson CL, *et al*.** Identification of GBF1 as a cellular factor required for hepatitis E virus RNA replication. *Cell Microbiol*. 2018;20:e12804.

8. **Claude A, Zhao BP, Kuziemsky CE, Dahan S, Berger SJ, *et al*.** GBF1: A novel Golgi-associated BFA-resistant guanine nucleotide exchange factor that displays specificity for ADP-ribosylation factor 5. *J Cell Biol*. 1999;146:71–84.

9. **Donaldson JG, Jackson CL.** ARF family G proteins and their regulators: roles in membrane transport, development and disease. *Nat Rev Mol Cell Biol*. 2011;12:362–375.

10. **Wright J, Kahn RA, Sztul E.** Regulating the large Sec7 ARF guanine nucleotide exchange factors: the when, where and how of activation. *Cell Mol Life Sci*. 2014;71:3419–3438.

11. **Bui QT, Golinelli-Cohen M-P, Jackson CL.** Large Arf1 guanine nucleotide exchange factors: evolution, domain structure, and roles in membrane trafficking and human disease. *Mol Genet Genomics*. 2009;282:329–350.

12. **Szul T, Grabski R, Lyons S, Morohashi Y, Shestopal S, *et al*.** Dissecting the role of the ARF guanine nucleotide exchange factor GBF1 in Golgi biogenesis and protein trafficking. *J Cell Sci*. 2007;120:3929–3940.

13. **Bouvet S, Golinelli-Cohen M-P, Contremoulins V, Jackson CL.** Targeting of the

Arf-GEF GBF1 to lipid droplets and Golgi membranes. *J Cell Sci*. 2013;126:4794–4805.

14. **Richards AL, Soares-Martins JAP, Riddell GT, Jackson WT**. Generation of unique poliovirus RNA replication organelles. *MBio*. 2014;5:e00833–13.

15. **Gazina EV, Mackenzie JM, Gorrell RJ, Anderson DA.** Differential requirements for COPI coats in formation of replication complexes among three genera of Picornaviridae. *J Virol*. 2002;76:11113–11122.

16. **Cherry S, Kunte A, Wang H, Coyne C, Rawson RB *et al.*** COPI activity coupled with fatty acid biosynthesis is required for viral replication. *PLoS Pathog*. 2006;2:e102.

17. **Tai AW, Benita Y, Peng LF, Kim S-S, Sakamoto N, *et al*.** A Functional Genomic Screen Identifies Cellular Cofactors of Hepatitis C Virus Replication. *Cell Host Microbe*. 2009;5:298–307.

18. **Wang J, Wu Z, Jin Q.** COPI is required for enterovirus 71 replication. *PLoS ONE*. 2012;7:e38035.

19. **de Wilde AH, Wannee KF, Scholte FEM, Goeman JJ, Dijke ten P, *et al*.** A Kinome-Wide Small Interfering RNA Screen Identifies Proviral and Antiviral Host Factors in Severe Acute Respiratory Syndrome Coronavirus Replication, Including Double-Stranded RNA-Activated Protein Kinase and Early Secretory Pathway Proteins. *J Virol*. 2015;89:8318–8333.

20. **Belov GA, Altan-Bonnet N, Kovtunovych G, Jackson CL, Lippincott-Schwartz J, *et al*.** Hijacking components of the cellular secretory pathway for replication of poliovirus RNA. *J Virol*. 2007;81:558–567.

21. **Matto M, Sklan EH, David N, Melamed-Book N, Casanova JE, *et al*.** Role for ADP Ribosylation Factor 1 in the Regulation of Hepatitis C Virus Replication. *J Virol*. 2011;85:946–956.

22. **Belov GA, Kovtunovych G, Jackson CL, Ehrenfeld E.** Poliovirus replication requires the N-terminus but not the catalytic Sec7 domain of ArfGEF GBF1. *Cell Microbiol*. 2010;12:1463–1479.

23. **Farhat R, Séron K, Ferlin J, Fénéant L, Belouzard S, *et al*.** Identification of class II ADP-ribosylation factors as cellular factors required for hepatitis C virus replication. *Cell Microbiol*. 2016;18:1121–1133.

24. **Farhat R, Goueslain L, Wychowski C, Belouzard S, Fénéant L, *et al*.** Hepatitis C virus replication and Golgi function in brefeldin a-resistant hepatoma-derived cells. *PLoS ONE*. 2013;8:e74491.

25. **Renault L, Guibert B, Cherfils J.** Structural snapshots of the mechanism and inhibition of a guanine nucleotide exchange factor. *Nature*. 2003;426:525–530.

26. **Sáenz JB, Sun WJ, Chang JW, Li J, Bursulaya B, *et al*.** Golgicide A reveals essential roles for GBF1 in Golgi assembly and function. *Nat Chem Biol*. 2009;5:157–165.

27. **Volpicelli-Daley LA, Li Y, Zhang C-J, Kahn RA.** Isoform-selective effects of the depletion of ADP-ribosylation factors 1-5 on membrane traffic. *Mol Biol Cell*. 2005;16:4495–4508.

28. **Kudelko M, Brault J-B, Kwok K, Li MY, Pardigon N, *et al.*** Class II ADP-ribosylation factors are required for efficient secretion of dengue viruses. *J Biol Chem*. 2012;287:767–777.

29. **Iglesias NG, Mondotte JA, Byk LA, De Maio FA, Samsa MM, *et al.*** Dengue Virus Uses a Non-Canonical Function of the Host GBF1-Arf-COPI System for Capsid Protein Accumulation on Lipid Droplets. *Traffic*. 2015;16:962–977.

30. **Reiling JH, Olive AJ, Sanyal S, Carette JE, Brummelkamp TR, *et al.*** A CREB3-ARF4 signalling pathway mediates the response to Golgi stress and susceptibility to pathogens. *Nat Cell Biol*. 2013;15:1473–1485.

31. **Dubuisson J, Hsu HH, Cheung RC, Greenberg HB, Russell DG, *et al.*** Formation and intracellular localization of hepatitis C virus envelope glycoprotein complexes expressed by recombinant vaccinia and Sindbis viruses. *J Virol*. 1994;68:6147–6160.

32. **Nakabayashi H, Taketa K, Miyano K, Yamane T, Sato J.** Growth of human hepatoma cells lines with differentiated functions in chemically defined medium. *Cancer Res*. 1982;42:3858–3863.

33. **Duvet S, Chirat F, Mir AM, Verbert A, Dubuisson J, *et al.*** Reciprocal relationship between alpha1,2 mannosidase processing and reglucosylation in the rough endoplasmic reticulum of Man-P-Dol deficient cells. *Eur J Biochem*. 2000;267:1146–1152.

34. **Thiel V, Herold J, Schelle B, Siddell SG.** Infectious RNA transcribed in vitro from a cDNA copy of the human coronavirus genome cloned in vaccinia virus. *J Gen Virol*. 2001;82:1273–1281.

35. **Engelmann I, Alidjinou EK, Bertin A, Bossu J, Villenet C, *et al.*** Persistent coxsackievirus B4 infection induces microRNA dysregulation in human pancreatic cells. *Cell Mol Life Sci*. 2017;74:3851–3861.

36. **Rouillé Y, Helle F, Delgrange D, Roingeard P, Voisset C, *et al.*** Subcellular localization of hepatitis C virus structural proteins in a cell culture system that efficiently replicates the virus. *J Virol*. 2006;80:2832–2841.

37. **Ran FA, Hsu PD, Wright J, Agarwala V, Scott DA, *et al.*** Genome engineering using the CRISPR-Cas9 system. *Nat Protoc*. 2013;8:2281–2308.

FIGURE LEGENDS

Figure 1. Brefeldin A sensitivity of viral infections. (a) Huh-7 cells were infected in the presence of indicated BFA concentrations. Infections were quantified by immunofluorescence assay and expressed as percentage of controls with no BFA. Error bars represent the standard deviation for 3 independent experiments. (b) Huh-7 cells were incubated with indicated BFA concentrations for 6h (BFA 6h) or for 8h followed by 22h without BFA (BFA 8h / DMEM 22h), and cell viability was assessed using an MTS assay. Error bars represent the standard deviation for 3 independent experiments. *, **, and *** mean p-values below .05, .01, and .001, respectively.

Figure 2. GBF1 requirement for viral infections. (a) R1 cells were infected in the presence of indicated BFA concentrations. Infections were quantified by immunofluorescence assay and expressed as percentage of controls with no BFA. Error bars represent the standard deviation for 3 independent experiments. (b) Huh-7 cells were infected in the presence of 50 μM GCA or 0.1% DMSO. Infections were quantified by immunofluorescence assay and expressed as percentage of DMSO controls. Error bars represent the standard deviation for 3 independent experiments. (c) Huh-7 cells were incubated with indicated GCA concentrations for 6h (GCA 6h) or for 8h followed by 22h without GCA (GCA 8h / DMEM 22h), and cell viability was assessed using an MTS assay. Error bars represent the standard deviation for 3 independent experiments. *, **, and *** mean p-values below .05, .01, and .001, respectively.

Figure 3. Brefeldin A inhibits a post-entry step. Huh-7 cells were infected in the presence of 1 μg/ml BFA or 0.02% DMSO during (entry) and/or after (post-entry) virus inoculation, as indicated. Infections were quantified by immunofluorescence assay and expressed as percentage of controls with no BFA. The data are the means of 2 independent experiments.

Figure 4. Impact of siRNA-mediated Arf depletion on viral infections. (a) Specificity of anti-Arf mAbs probed on lysates of Huh-7 cells expressing the proteins indicated above the blots. (b, c) Specificity of siRNA-mediated depletions. Huh-7 cells were transfected with indicated siRNAs. Arf proteins expression was monitored by immunoblotting at 3 days post-transfection (b), and the bands were quantified (c). Results are expressed as percentages of control non-targeting (siNT1) siRNA. Error bars represent the standard deviation for 3 independent experiments. (d, e) Huh-7 cells were transfected with indicated siRNAs (d) or siRNA pairs (e) and infected at 3 days post-transfection. Infections were quantified by immunofluorescence assay and expressed as percentage of control siNT1-transfected cells. Error bars represent the standard deviation for 6 independent experiments. (f) Cell viability of siRNA-transfected Huh-7 cells probed at 3 days post-transfection using an MTS assay and expressed as a percentage of control siNT1-transfected cells. Error bars represent the standard deviation for 3 independent experiments. *, **, and *** mean p-values below .05, .01, and .001, respectively. (g) Huh-7 cells were transfected with indicated siRNA pairs and infected with CVB4 at 3 days post-transfection. The expression of VP1, Arf proteins and tubulin was monitored by immunoblotting.

Figure 5. Viral infections of ArfKO cell lines. Arf5KO (5.1), Arf4KO (4.1) and Arf1KO (1.1; 1.2 and 1.3) cell lines were generated using the CRISPR-Cas9 technology. A control cell line was generated with no sgRNA. (a, b) Arf proteins expression was monitored by immunoblotting (a) and the bands were quantified (b). Results are expressed as percentages relative to the control cell line. The data are the means of 2 independent experiments. (c) KO cells were infected with indicated viruses. Infection were quantified by immunofluorescence

590 assay and expressed as percentage of control KO cells. The data are the means of 2
591 independent experiments.
592
593 **Figure 6. Impact of siRNA-mediated Arf4 depletion in Arf5KO cells on viral infections.**
594 Control and Arf5KO cell lines were transfected with siRNAs to Arf4 or Arf5 or control non-
595 targeting siNT1. At 3 days post-transfection, (a) the cell viability was measured using an
596 MTS assay, (b) Arf4 and Arf5 expression was monitored by immunoblotting, and (c) the cells
597 were infected with indicated viruses. Infections were quantified by immunofluorescence assay
598 and expressed as percentage of control siRNA (NT1)-transfected control cells. Error bars
599 represent the standard deviation for 3 independent experiments. *, **, and *** mean p-values
600 below .05, .01, and .001, respectively.
601

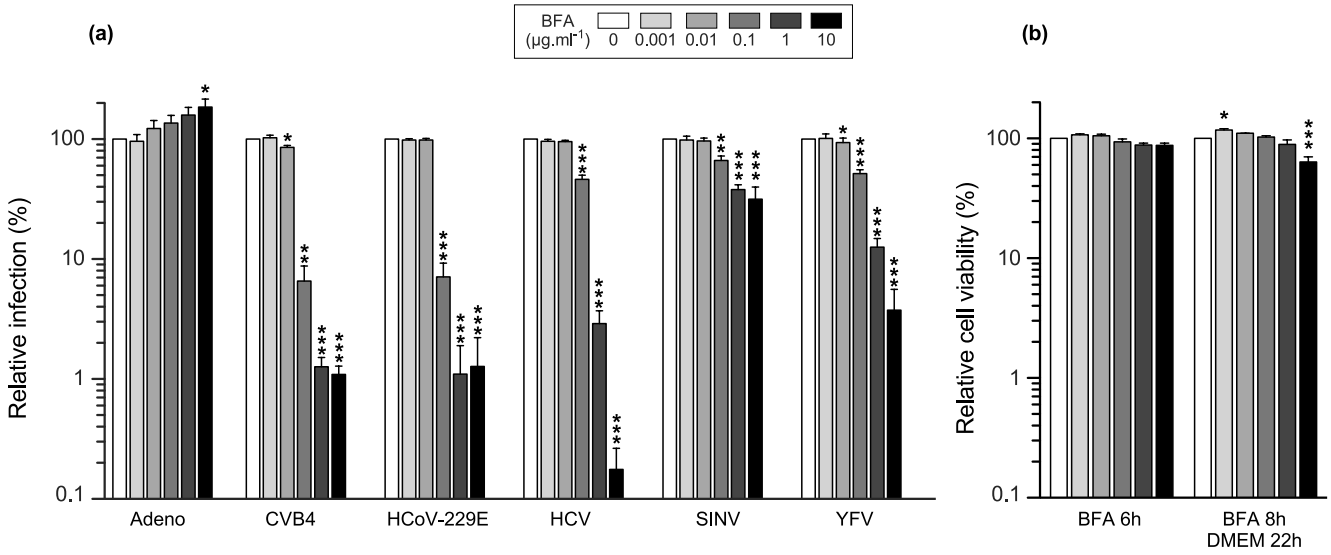
(a)
BFA (µg.ml-1) 0 0.001 0.01 0.1 1 10
Relative infection (%)
100
10
1
0.1
Adeno
CVB4
HCoV-229E
HCV
SINV
YFV
(b)
Relative cell viability (%)
100
10
1
0.1
BFA 6h
BFA 8h DMEM 22h

Figure 1

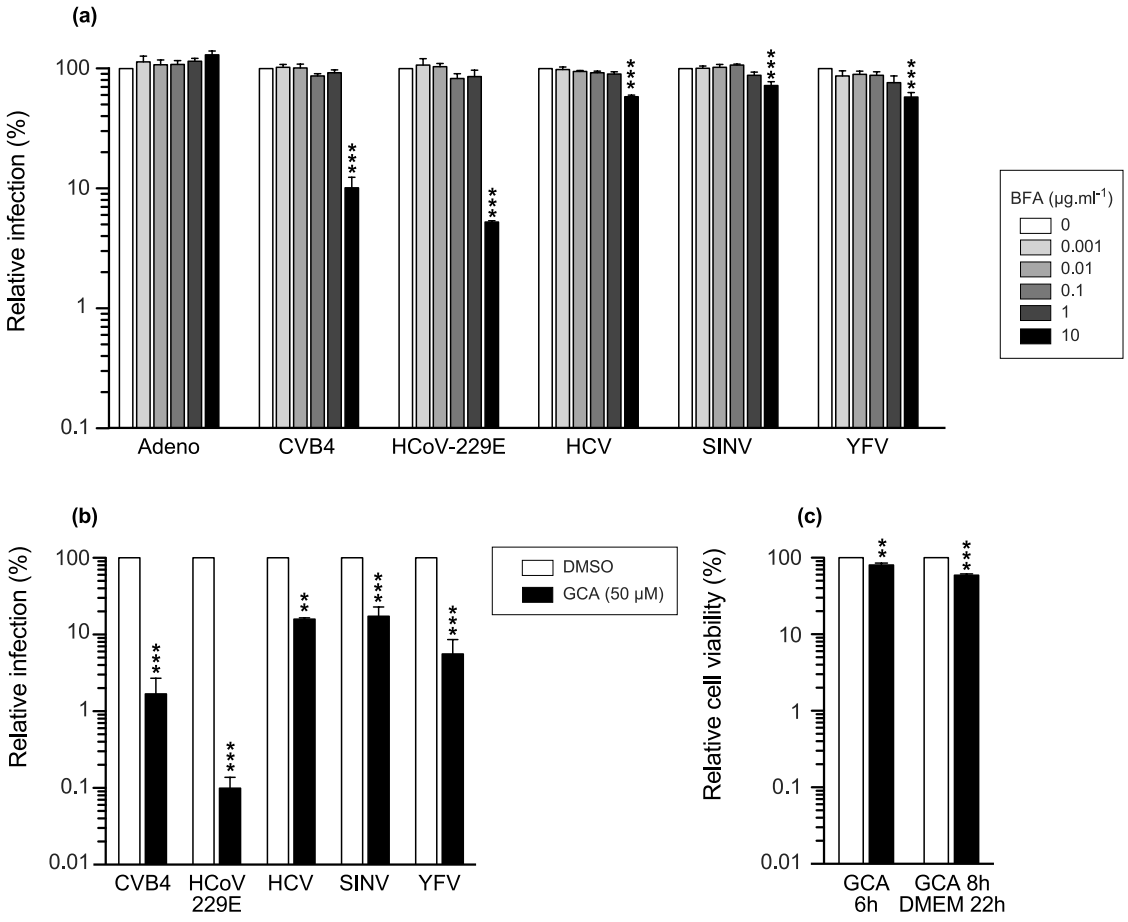
(a)
Relative infection (%)
100
10
1
0.1
Adeno
CVB4
HCoV-229E
HCV
SINV
YFV
BFA (µg.ml-1)
0
0.001
0.01
0.1
1
10
(b)
Relative infection (%)
100
10
1
0.1
0.01
CVB4
HCoV 229E
HCV
SINV
YFV
DMSO
GCA (50 µM)
(c)
Relative cell viability (%)
100
10
1
0.1
0.01
GCA 6h
GCA 8h DMEM 22h

Figure 2

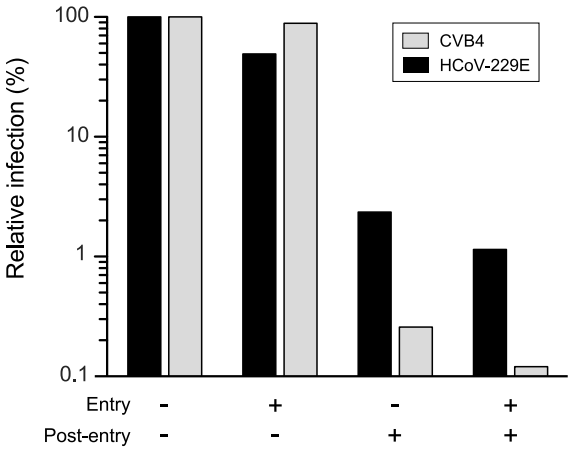
100
10
1
0.1
Relative infection (%)
CVB4
HCoV-229E
Entry - + - +
Post-entry - - + +

Figure 3

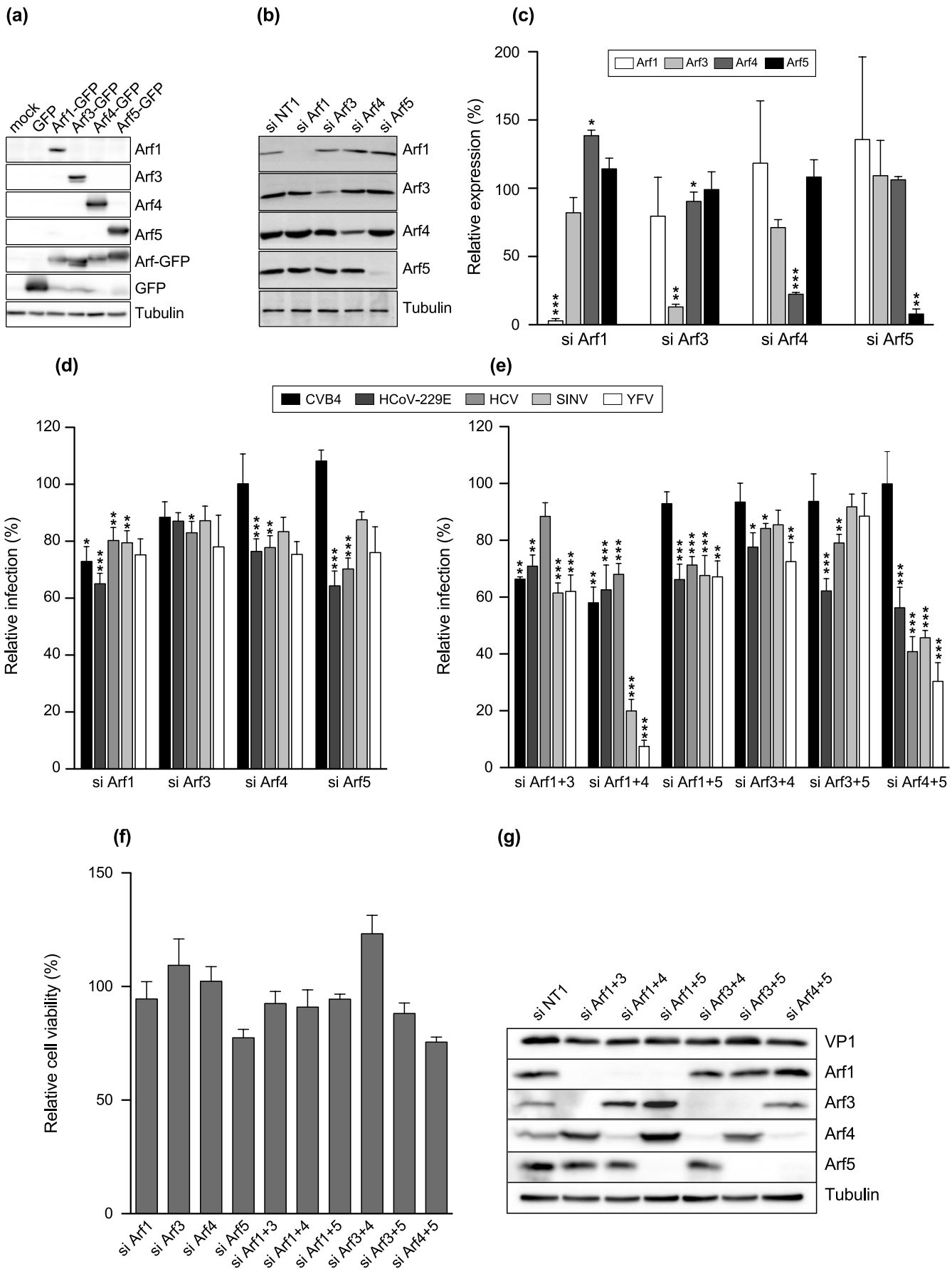
(a)
mock
GFP
Arf1-GFP
Arf3-GFP
Arf4-GFP
Arf5-GFP
Arf1
Arf3
Arf4
Arf5
Arf-GFP
GFP
Tubulin
(b)
si NT1
si Arf1
si Arf3
si Arf4
si Arf5
Arf1
Arf3
Arf4
Arf5
Tubulin
(c)
Arf1
Arf3
Arf4
Arf5
Relative expression (%)
200
150
100
50
0
si Arf1
si Arf3
si Arf4
si Arf5
(d)
CVB4
HCoV-229E
HCV
SINV
YFV
Relative infection (%)
120
100
80
60
40
20
0
si Arf1
si Arf3
si Arf4
si Arf5
(e)
Relative infection (%)
120
100
80
60
40
20
0
si Arf1+3
si Arf1+4
si Arf1+5
si Arf3+4
si Arf3+5
si Arf4+5
(f)
Relative cell viability (%)
150
100
50
0
si Arf1
si Arf3
si Arf4
si Arf5
si Arf1+3
si Arf1+4
si Arf1+5
si Arf3+4
si Arf3+5
si Arf4+5
(g)
si NT1
si Arf1+3
si Arf1+4
si Arf1+5
si Arf3+4
si Arf3+5
si Arf4+5
VP1
Arf1
Arf3
Arf4
Arf5
Tubulin

Figure 4

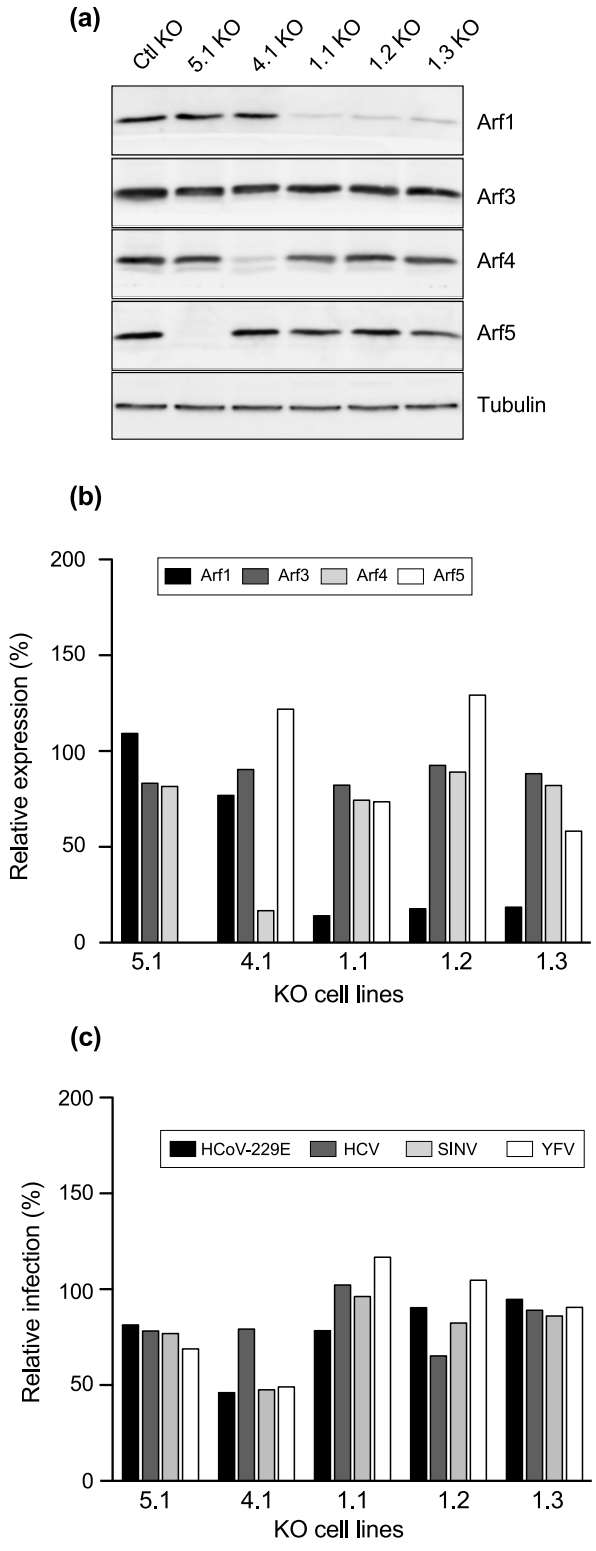
(a)
Ctl KO
5.1 KO
4.1 KO
1.1 KO
1.2 KO
1.3 KO
Arf1
Arf3
Arf4
Arf5
Tubulin
(b)
Arf1
Arf3
Arf4
Arf5
Relative expression (%)
200
150
100
50
0
5.1
4.1
1.1
1.2
1.3
KO cell lines
(c)
HCoV-229E
HCV
SINV
YFV
Relative infection (%)
200
150
100
50
0
5.1
4.1
1.1
1.2
1.3
KO cell lines

Figure 5

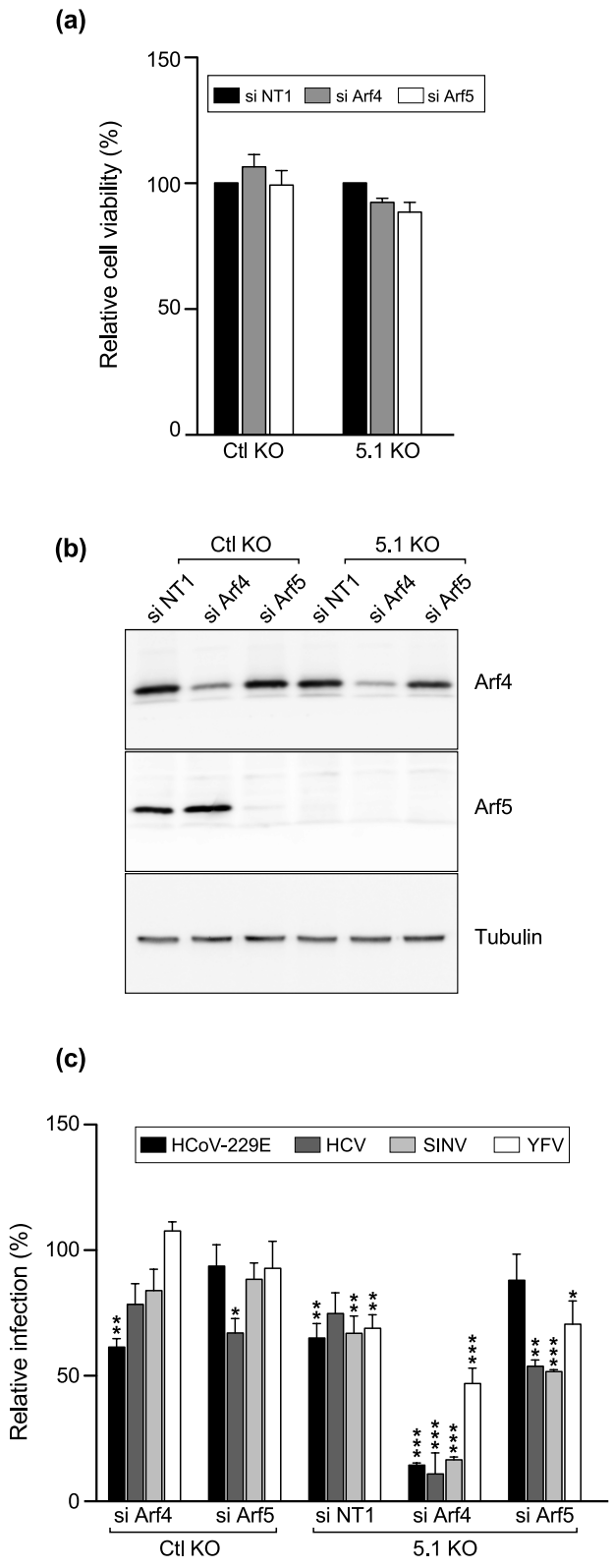
(a)
150
100
50
0
Relative cell viability (%)
si NT1
si Arf4
si Arf5
Ctl KO
5.1 KO
(b)
Ctl KO
5.1 KO
si NT1
si Arf4
si Arf5
si NT1
si Arf4
si Arf5
Arf4
Arf5
Tubulin
(c)
150
100
50
0
Relative infection (%)
HCoV-229E
HCV
SINV
YFV
si Arf4
si Arf5
si NT1
si Arf4
si Arf5
Ctl KO
5.1 KO

Figure 6